Technical Aspects of Cardiorespiratory Estimation Using Subspace Projections and Cross Entropy

John Morales[1,2], Jonathan Moeyersons[1,2], Dries Testelmans[3], Bertien Buyse[3], Pascal Borzée[3], Chris Van Hoof[4], Willemijn Groenendaal[5], Sabine Van Huffel[1,2], Carolina Varon[1]

[1] ESAT - STADIUS, Stadius Centre for Dynamical Systems, Signal Processing and Data Analytics, KU Leuven, 3001 Leuven, Belgium.

[2] KU Leuven institute for AI, KU Leuven, 3001 Leuven, Belgium.

[3] Department of Pneumology, UZ Leuven, Leuven, Belgium.

[4] Imec, Leuven, Belgium.

[5] Imec the Netherlands/Holst Centre, Eindhoven, The Netherlands.

E-mail: `jmorales@esat.kuleuven.be`

April 2021

Abstract. *Background:* Respiratory sinus arrhythmia (RSA) is a form of cardiorespiratory coupling. Its quantification has been suggested as a biomarker to diagnose different diseases. Two state-of-the-art methods, based on subspace projections and entropy, are used to estimate the RSA strength and are evaluated in this paper. Their computation requires the selection of a model order, and their performance is strongly related to the temporal and spectral characteristics of the cardiorespiratory signals. *Objective:* To evaluate the robustness of the RSA estimates to the selection of model order, delays, changes of phase and irregular heartbeats as well as to give recommendations for their interpretation on each case. *Approach:* Simulations were used to evaluate the model order selection when calculating the RSA estimates introduced before, as well as 3 different scenarios that can occur in signals acquired in non-controlled environments and/or from patient populations: the presence of irregular heartbeats; the occurrence of delays between the heart rate variability (HRV) and respiratory signals; and the changes over time of the phase between the HRV and respiratory signals. *Main results:* It was found that using a single model order for all the calculations suffices to characterize the RSA correctly. In addition, the estimation of the RSA in signals containing more than 5 irregular heartbeats in a period of 5 minutes might be misleading. Regarding the delays between the HRV and respiratory signals, both estimates are robust. For the last scenario, the two approaches tolerate phase changes up to 54°, as long as this lasts less than one fifth of the recording duration. *Significance:* Guidelines are given to compute the RSA estimates in non-controlled environments and patient populations.

Keywords: cardiorespiratory coupling, respiratory sinus arrhythmia, heart rate

1. Introduction:

The respiratory sinus arrhythmia (RSA) is a form of synchronization between the cardiac and the respiratory systems. It is characterized by an increased heart rate (HR) during inhalation and a decreased HR during exhalation. The RSA is hypothesized to be an indicator of the efficiency of the cardiorespiratory system and has been suggested as a biomarker for diseases such as diabetes or sleep apnea as well as for conditions like stress, or anxiety [1, 2, 3, 4, 5, 6]. For this reason, the development of methods for RSA estimation is an active research topic.

The RSA is commonly evaluated using a heart rate variability (HRV) representation [7], which can be derived from cardiac signals, such as the electrocardiogram (ECG) or the photoplethysmogram. The most widely used method to assess the RSA is based on the analysis of the power spectral density of the HRV. Here, it is assumed that the respiratory modulations act in the high frequency band (HF: 0.15-0.4 Hz) [8]. However, different studies suggest that this interpretation might be misleading in cases in which the respiratory rate falls outside this band [9, 10, 11, 12]. For this reason, alternative approaches that take into account the respiratory signal have been recently proposed. Seven of them were compared in [13] using a simulation model. This comparison highlighted the advantages of orthogonal subspace projections [6] and cross entropy [14] for the estimation of the RSA.

Despite their good performance, these two methods have been mostly studied under controlled conditions and using signals from healthy subjects. Furthermore, they require the tuning of a model order, whose selection might significantly affect the outcomes of the calculations. For these reasons, it is needed to understand the effect of the model order as well as the interpretation of the results in patient populations and in non-controlled environments. In this context, the current paper assesses the aforementioned RSA estimates using simulated data. First, the tuning of the model order is evaluated. Next, three scenarios hypothesized in previous works to have an impact in the estimation of the RSA are assessed, i.e. when irregular heartbeats appear, when delays between the signals exist and when phase shifts occur.

First, the effect of the model order selection on the RSA estimates is studied. It is not well understood how this selection affects the results and it is hypothesized to depend on the spectral characteristics of the respiratory signals [6]. After understanding this selection, three scenarios are assessed. The first one evaluates the RSA estimates when different number of irregular heartbeats occur. Irregular heartbeats are commonly observed in recordings from people with diseases such as diabetes [16] or cardiac comorbidities related to sleep apnea [17]. Guidelines for a correct RSA estimation in these cases have not been given yet while irregular heartbeats are known to affect the reliability of HRV-based analyses [15]. The second scenario focuses on the possible delays between the signals. Respiratory recordings acquired or derived from different modalities might be delayed differently with respect to the HRV due to the hardware used to acquire the signal, to the processing methods or to the physical characteristics

of the subjects [18]. The third and last scenario considers continuous phase changes between the respiration and the HRV. It has been suggested that this phase is not constant [19], and different patient populations show different phase patterns over time [20, 21, 22].
With the results, guidelines for using the RSA estimates in future applications are given. This paper is organized as follows. The methods and performed simulations are described in Section 2. Section 3 and 4 show the results and discusses them, respectively. Finally, section 4 gives the conclusions.

2. Materials and Methods

2.1. RSA estimators

According to [13], cross entropy and orthogonal subspace projections outperformed other established methodologies for RSA estimation.

2.1.1. Cross Entropy: The crossentropy (CE) [14] is a term based on information theory that is often used to estimate the interaction between the cardiac and the respiratory systems. CE quantifies the information in the present samples of the HRV shared with the past of the respiration, which can be achieved by means of a multivariate autoregressive (MVAR) model. To derive this model, the respiratory time-series, $x_1(n)$, and the HRV times-series, $x_2(n)$, are put together in a vector, $\mathbf{x}(n) = [x_1(n)\ x_2(n)]^T$ where $n = 1 : N$, and N is the total number of samples. The nth sample in $\mathbf{x}(n)$ can be estimated as a linear combination of q past samples as,

$$\mathbf{x}(n) = \sum_{k=1}^{q} \mathbf{A}(k)\mathbf{x}(n-k) + \mathbf{w}(n), \tag{1}$$

where $\mathbf{A}(k)$ is a matrix of regression coefficients, $\mathbf{w}$ contains two independent residual noises, and q is the model order. This equation is solved for $\mathbf{A}(k)$, which contains the coefficients of different regressions between the signals and their past samples. The residuals of these regressions serve to estimate the CE.
Assuming that the processes follow a Gaussian distribution and that their interactions are linear, the following equation can be used to estimate the CE,

$$CE = \frac{1}{2} \ln \left(\frac{\sigma^2(x_2)}{\sigma^2(x_2 \mid x_1^-)} \right), \tag{2}$$

where x_1^- corresponds to the past samples of the respiration up to $N - q$. $\sigma^2(x_2)$ is the variance of the HRV, and $\sigma^2(x_2 \mid x_1^-)$ is the partial variance of x_2 given x_1^- or, in other words, the variance of the residuals of the regression in which the past samples of the respiration are used as regressor for the present samples of the HRV.

2.1.2. Orthogonal subspace projections: This approach measures the proportion of variance in the HRV linearly correlated with the respiration [6]. To compute it, an

embedding ($\mathbf{V}$) of the respiratory signal, with dimension q is generated. $\mathbf{V}$ is used to build a projection matrix $\mathbf{P}$ as,

$$\mathbf{P} = \mathbf{V}(\mathbf{V}^T\mathbf{V})^{-1}\mathbf{V}^T. \tag{3}$$

The product between $\mathbf{P}$ and the HRV results in a time series representing the dynamics in the HRV linearly correlated with the respiration as,

$$\hat{x}_{2_R} = \mathbf{P}\hat{x}_2, \tag{4}$$

where $\hat{x}_2$ contains the samples in x_2 from 1 to $N - q$. The proportion of variance in the HRV linearly correlated with the respiration is then computed as,

$$\mathcal{P}_x = \frac{\hat{x}_{2_R}\hat{x}_{2_R}^T}{\hat{x}_2\hat{x}_2^T}. \tag{5}$$

2.2. Datasets

Two datasets generated with different approaches are used. The first one contains HRV signals calculated with the simulation shown in Figure 1. This model uses a respiratory segment and a noise signal as inputs. These are multiplied by a coefficient, which represents the strength of the coupling, and added to produce a modulating signal. With this, a train of pulses representing the heartbeats is constructed. The points in time in which these pulses occur are defined by the modulating signal. Next, the HRV is calculated and it is then used in combination with the respiration to compute the RSA estimates. The motivation to use this dataset was to study the effect of the model order selection while knowing the actual coupling levels. The second dataset consisted of 5-minutes clean respiratory and HRV epochs taken from a dataset of sleep apnea patients. Actual recordings were used here to have signals with coupling characteristics that would occur in real life. Both datasets are explained in more detail next.

2.2.1. Simulated Data: The model shown in Figure 1 was used to generate HRV and respiratory signals with different coupling levels [13]. In this model, a modulating signal ($m(t)$) with a sampling frequency of 1000 Hz is built as the addition of two components, one due to non-respiratory modulators ($m_C(t)$) and a second one due to the respiratory modulation ($m_R(t)$) of the heart rate. A sampling frequency of 1000 hz was chosen to have enough time resolution in the simulation. To create $m_C(t)$, a filter was built with the coefficients of an autoregressive model made using an HRV signal obtained from a healthy subject during the tilt test described in [23]. These coefficients were modified to remove the peak in the HF band, which is mainly due to the respiration. A Gaussian noise epoch was generated (fs=1 Hz), filtered with the aforementioned filter and then upsampled to 1000 Hz to obtain $m_C(t)$.

For $m_R(t)$, a dataset of 2459 5-minute respiratory segments was available. It was built using the thoracic respiratory recording from three datasets. The first one was the Fantasia dataset (fs=250 Hz), available in Physionet [24] and acquired from 40 healthy volunteers. The second one was the stress recognition in the automobile drivers' dataset

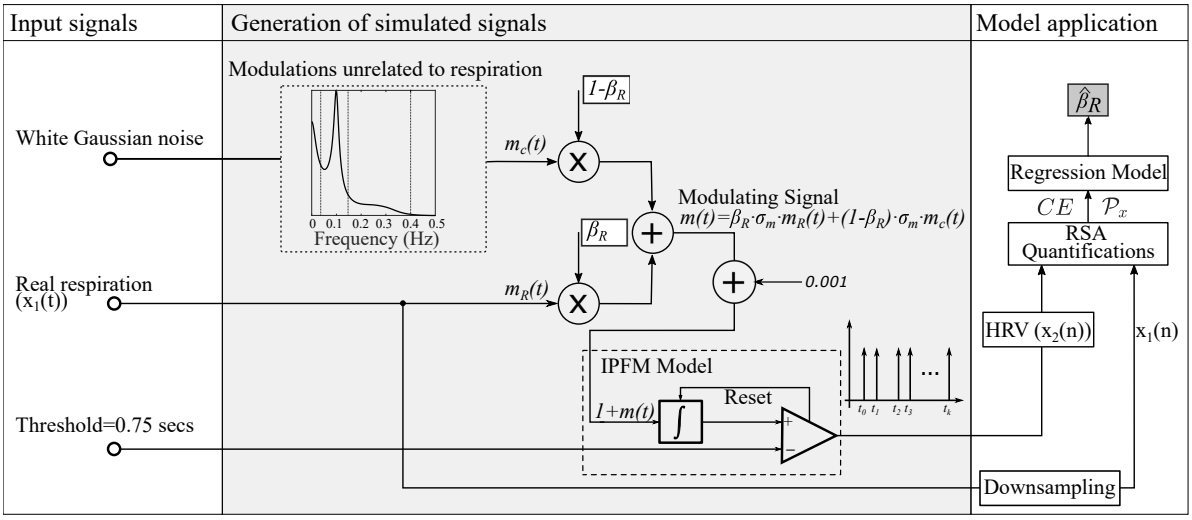

Figure 1. Model used to generate the simulated signals. The inputs are a white gaussian noise and a real respiratory segment. Both serve to create $m(t)$, in which a coefficient β_R simulates the coupling strength. $m(t)$ is integrated in the IPFM model, which fires a pulse when this integral reaches a threshold. These pulses simulate the R-peaks locations. Adapted from [13].

(fs=31 Hz), also from Physionet [25] and acquired from 16 healthy volunteers. The third one was recorded in the university hospitals UZ Leuven from 110 sleep apnea patients (fs=500 Hz) and is not publicly available [26]. In the latter, segments with apneas were eliminated. Three datasets were used to consider respiratory segments with different spectral characteristics. Taking into account the sampling frequency on each case, the signals were filtered to preserve frequency components between 0.03 and 0.9 Hz with a Butterworth filter in forward and backward direction to have zero-phase distortions, upsampled to 1000 Hz and then segmented into 5-minutes epochs. Next, these segments were visually divided into two groups: regular and irregular, according to their spectral characteristics, using the following rules: if the spectrum had a clearly defined peak, it was classified as regular; otherwise, it was classified as irregular; segments contaminated with artifacts were eliminated [13]. $m_R(t)$ is a signal randomly taken from this dataset. After obtaining the two components, these are normalized and $m(t)$ is calculated as,

$$m(t) = \beta_R \sigma_m m_R(t) + (1 - \beta_R)\sigma_m m_C(t), \tag{6}$$

where β_R represents the strength of the RSA and σ_m is the standard deviation of the modulating signal. For the sinoatrial node to work, its membrane potential has to increase over time [27] and, when a threshold is reached, a pulse is fired. To model this phenomena, the integral pulse frequency modulation (IPFM) model can be used. This model was chosen since it has been widely studied and validated to assess the properties of biomedical signals. The signal $m(t)$ is fed into the IPFM model, which integrates its input over time [28] and when the integral reaches a threshold, a unitary pulse is fired, the integral is reset to zero and the integration starts again. The resulting pulses represent the locations of the R-peaks in an ECG signal modulated by $m(t)$. With the

time locations of these pulses, the RR-interval time-series is generated, which is then interpolated with a spline to a constant sampling frequency of 4 Hz. This is used as the HRV representation. The HRV and the respiratory segments serve to estimate the RSA strength using $\mathcal{P}_x$ and CE. Next, the values of $\mathcal{P}_x$ and CE are used to obtain $\hat{\beta}_R$ with regression models [13]. $\hat{\beta}_R$ is an estimation of the "real" coupling value given by β_R.
To generate the dataset of simulated signals, β_R was varied from 0.05 to 0.95 in steps of 0.1. Afterwards, 50 simulated signals were generated for each β_R. It is hypothesized that a higher model order is needed when irregular respiratory signals are used to calculate the RSA estimates. For this reason, the simulations were repeated twice with either the regular or the irregular respiratory segments each time.

2.2.2. Real Data: The used dataset was recorded in the University Hospitals Leuven (UZ Leuven), Belgium from 110 patients referred to the sleep laboratory [26]. The recording of the data and its inclusion in this study was approved by the ethical committee of the hospital (S53746, S60319). Polysomnographic recordings were acquired, from which lead V1 ECG and thoracic respiratory signals recorded with inductance plethysmography, both sampled at 500 Hz, were extracted. From the ECG signals, the R-peaks were detected with the method proposed in [29] and then used to build the RR-intervals time-series. Afterwards, this was interpolated to a sampling frequency of 4 Hz to create a uniformly sampled HRV representation. Next, the HRV was filtered with a 4th order buttterworth filter in forward and backward direction to preserve frequency components between 0.03 and 1 Hz. The respiratory signals were first bandpass-filtered in the same way as with the HRV and then downsampled to 4 Hz. The resulting HRV and respiratory signals were segmented into 5-minutes epochs. Segments with apneas were discarded using the annotations given by the doctors based on the AASM 2012 scoring rules [30]. Furthermore, a visual selection was done to remove segments with contaminated recordings or ECG signals with irregular heartbeats.
The cardiorespiratory coupling was estimated in the remaining segments using the approach described in section 2.1.2. The obtained coupling value was used to divide the segments in ten groups according to their $\mathcal{P}_x$ level, from 0 to 1 in intervals of 0.1. Finally, 50 segments per group were chosen at random. As a result of this procedure, a dataset of clean HRV and respiratory signals with a known coupling value was obtained. At this point, it is worth mentioning that the objective was to obtain a dataset of clean epochs with known coupling. These were contaminated later on to simulate the scenarios mentioned in the introduction. The dataset presented in this section corresponds to the dataset 1 described in [31].

2.3. Technical aspects and experiments

2.3.1. Model order selection: An open problem in the quantification of the cardiorespiratory coupling using $\mathcal{P}_x$ and CE is the selection of the model order, q. For CE, q is the number of past samples to build the MVAR model. For $\mathcal{P}_x$, it is the

dimension to construct the embedding of the respiration. In both cases, q determines the time-scale of the dynamics captured by the RSA estimates. Some approaches exist for this selection, but they are not robust when applied to different problems. For the specific case of the evaluation of the cardiorespiratory coupling, the need to standardize this selection is highlighted in [32]. Two methods frequently used in literature were compared in this paper, namely, the Akaike's information criterion (AIC) [33] and the minimum description length (MDL) [34] criterion. In addition, the empirical approach proposed in [13], used specifically for cardiorespiratory analysis, was evaluated. To obtain the model order with this approach, the PSD estimation of the respiration was calculated using the Welch's algorithm with a Hanning window of 40 seconds and 20 seconds overlap. Afterwards, the 90% occupied bandwidth was identified and the modes in this band were analyzed to decide the best model order. If the number of modes was lower than 3, q was defined as the number of samples needed to capture two periods of the frequency (F_r) corresponding to the maximum mode in terms of power. If the number of modes was higher than 3, q was the number of samples needed to capture two periods of the F_r of the first mode. However, if $F_r < 0.1$, it was chosen as 0.1.

Experiment: In order to understand the effect of the model order selection, the simulated signals described in 2.2.1 were used. The coupling was estimated 60 times on each pair of epochs with a model order between 2 and 120 in steps of 2. Hence, 3000 RSA estimates were computed per coupling level with different model orders, to sum up 30000 samples. Afterwards, the regression models were used to find $\hat{\beta}_R$, which is an estimation of the "real" coupling value, β_R. The goal was to evaluate the model orders that resulted in a consistent $\hat{\beta}_R$. In addition, the model orders obtained with MDL, AIC and the empirical approach were calculated and compared.

2.3.2. Effect of irregular beats: It is well-known that the HRV indices are affected by the presence of irregular heartbeats [15]. As a consequence, it is expected that the estimation of the RSA is also affected. However, the extent in which this occurs, and the number of tolerated irregular beats is not yet known.

Experiment: The RR-interval times series from the segments described in section 2.2.2 were contaminated with artificially generated irregular beats using the following expressions [15],

$$RR'_n = \gamma RR_{n-1}, \qquad RR'_{n+1} = RR_{n+1} - RR'_n, \tag{7}$$

where the RR_n and RR_{n+1} intervals are modified to RR'_n and RR'_{n+1}, respectively, by slightly changing their length. Here, γ is a random value in the interval [0.3 0.8], and determines the amount of time that a randomly chosen R-peak is delayed or advanced with respect to the actual one [35]. RR' are the simulated irregularities in the RR-intervals. The available segments were contaminated 25 times with an increasing number of simulated ectopic beats each time. An example of an HRV before and after

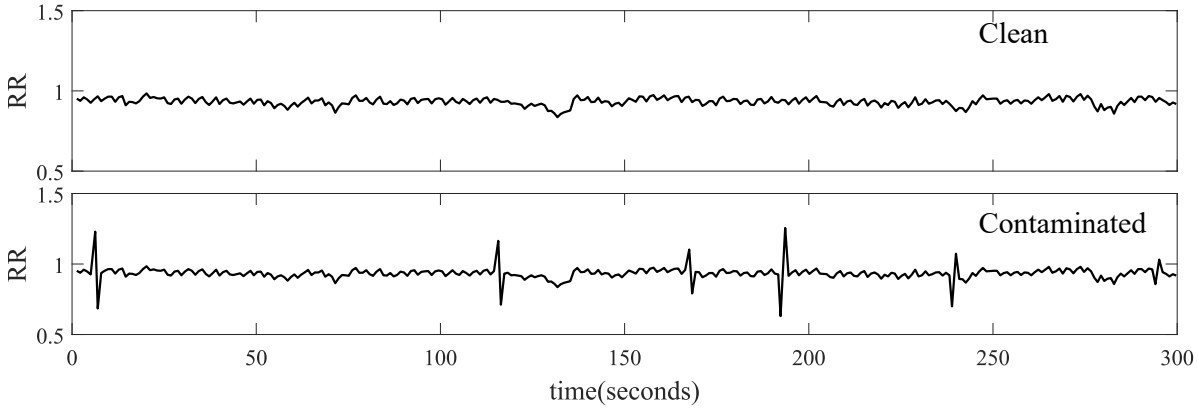

Figure 2. An example of an HRV signal in which 6 simulated irregular beats are added.

contamination is shown in figure 2.

Afterwards, the simulated irregular beats were corrected. For this, the derivative of the HRV was calculated and a threshold was defined by visual inspection. In cases in which the derivative was higher than the threshold, an irregularity was detected. Next, an interpolation was done between one point before and one point after the detected irregularity. A single threshold was used for the whole dataset since the HRV representations had similar characteristics, therefore one threshold worked properly for all of them. The RSA was estimated using the contaminated as well as the corrected HRV signals.

2.3.3. Effect of delays between the signals: Different respiratory signals can be used to estimate the cardiorespiratory coupling. Examples include belts, pressure sensors, temperature sensors, bioimpedance sensors or the ECG derived respiration. Depending on the used signals, the delay between the HRV and respiration might be different [18]. The effect of this delay on the RSA estimates has not been investigated.

Experiment: To evaluate this effect, the respiratory signals from the segments described in 2.2.2 were delayed by up to 7.5 seconds (30 samples) with respect to the HRV, and $\mathcal{P}_x$ as well as CE were calculated for each case.

2.3.4. Effect of phase changes: In [36], it was suggested that the phase between breathing and HRV might not be constant. A moderate significant linear correlation between phase and age (20-60 y.o.) was found, in which younger subjects tended to present phases closer to 180°. This means that the trend towards an increased HR during inhalation and a decreased one during exhalation is less pronounced in the elder. This is also the underlying reason to hypothesize the existence of another form of cardiorespiratory coupling, the cardiorespiratory phase synchronization [37]. It is said that a phase locking between the heartbeats locations and respiratory signals occurs and changes over time. The amount of time in which this synchronization remains constant

has been used as a biomarker for different conditions [20].
From equations 2 and 5, it is inferred that $\mathcal{P}_x$ and CE are only able to capture instantaneous and linear interactions. When the phase between the signals changes in a recording under analysis, this condition is not met and $\mathcal{P}_x$ as well as CE fail to reflect the actual coupling strength. The extend in which this occurs has not been investigated.

Experiment: To simulate this effect, the Hilbert transform (HT) was used. Given a respiratory signal, $x_1(t)$, its HT is defined as,

$$y(t) = \frac{1}{\pi} C \int_{-\infty}^{\infty} \frac{x_1(t')}{t - t'} dt', \tag{8}$$

where C is the Cauchy principal value. The sampled version of $y(t)$, $y(n)$, can be found with the discrete fourier transform, as explained in [38]. Using $y(n)$, the analytical function $z(n)$ is defined as,

$$z(n) = x_1(n) + iy(n) = B(n)e^{i\phi(n)}, \tag{9}$$

with the following amplitude ($B(n)$) and instantaneous phase ($\phi(n)$),

$$B(n) = \sqrt{x^2(n) + y^2(n)}, \tag{10}$$

$$\phi(n) = \tan^{-1}\left(\frac{y(n)}{x(n)}\right). \tag{11}$$

The analytical time series of the respiratory segments extracted in 2.2.2 were calculated with equation (9). Afterwards, $\phi(n)$ was derived using equation (11) and then modified by adding a pulse function. The duration of this pulse was varied between 20 seconds and 160 seconds, in steps of 20 seconds. A linear increase or decrease before and after the pulse were added to have a smooth change of phase. In addition, the amplitude of the pulse was varied in 10 uniformly separated steps between 0 and 180°. These pulses were added to the original $\phi(n)$ to generate a new phase, $\phi'(n)$. This new phase, together with $B(n)$ were used to generate a new analytical function $z'(n) = B(n)e^{i\phi'(n)} = x'(n)+iy'(n)$. As a result, $x'(n)$ corresponds to a phase-changed respiratory signal. An example is shown in figure 3, where a phase change of 180° for 3 minutes was introduced.

2.4. Analysis

The RSA estimates were hypothesized to change with different model orders and in each simulated scenario. They were expected to increase with an increased model order, to decrease with an increased number of irregulars, to decrease with an increased delay and to decrease with stronger and longer phase changes.
To evaluate these, two analyses were performed. First, Bland-Altman plots [39] were used to verify the change under the simulated conditions with respect to the originally calculated values. Second, differences between the clean cases and the simulated ones were evaluated using Kruskal-Wallis tests with Bonferroni correction, considering a $\mathbf{p} < 0.05$ as significant.

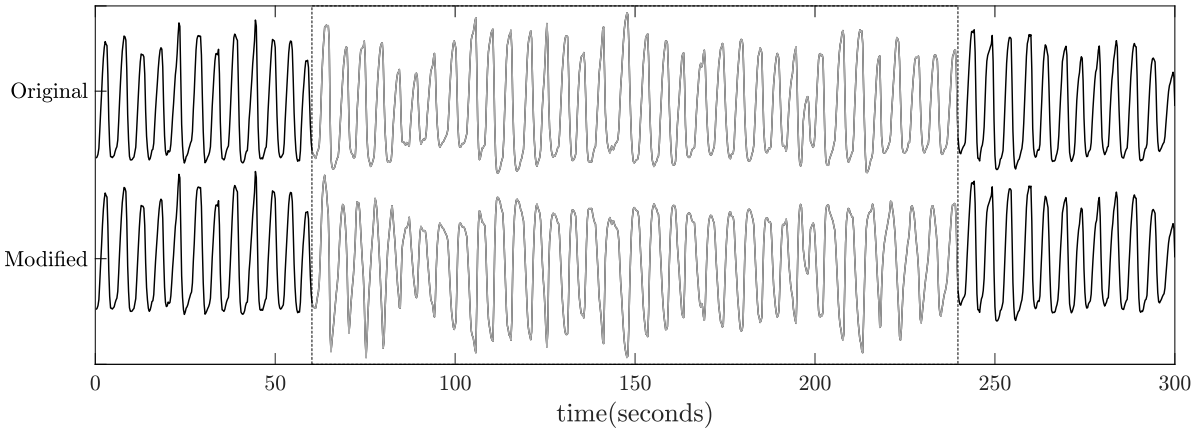

Figure 3. An example of a respiratory segment before and after changing its instantaneous phase. In gray, portion of the signal in which a phase shift of 180° is done.

3. Results

3.1. Model order selection

Figures 4(a) and 4(b) show the results of the estimation of the RSA using $\mathcal{P}_x$ when the model order in samples is varied from 2 to 120, and using either regular or irregular respiratory segments, respectively. These plots were made for the signals sampled at 4 Hz. Hence, the simulated model orders correspond to 0.25 to 30 seconds. Different aspects can be highlighted here. First, the interquartile range (IQR) of the estimates is wider when irregular respiratory signals are used. For instance, when $\beta_R = 0.25$, the average IQR is 0.034 and 0.051, when using regular and irregular respiratory segments, respectively. Furthermore, the selection of q needs to be carefully done when a weak coupling is expected. In such cases, the use of a high model order is not advisable because $\mathcal{P}_x$ is not able to distinguish between similar coupling levels. On the other hand, when the actual coupling is stronger ($\beta_R > 0.35$), the model order does not have an important impact on the calculations.

Figures 4(c) and 4(d) show the results of the RSA estimation for different model orders with CE, using regular and irregular respiratory segments, respectively. It is observed that the IQR of the quantification with irregular respiratory signals is broader when β is below 0.4. For instance, when $\beta_R = 0.25$, the average IQR is 0.042 and 0.060, when using regular and irregular respiratory segments, respectively. In addition, a model order below 5 samples might produce inconsistent estimations. This is observed in the figure as values higher than the expected β_R. However, above $q = 5$, an accurate estimation is achieved.

In order to confirm if the RSA estimates with model orders higher than 8 were significantly different to the results with 8 samples, Bland-Altman plots were used. A $q = 8$ was chosen since, from figure 4, it is observed that this value produces consistent estimates with both approaches. Figure 5 illustrates the results, in which it is observed

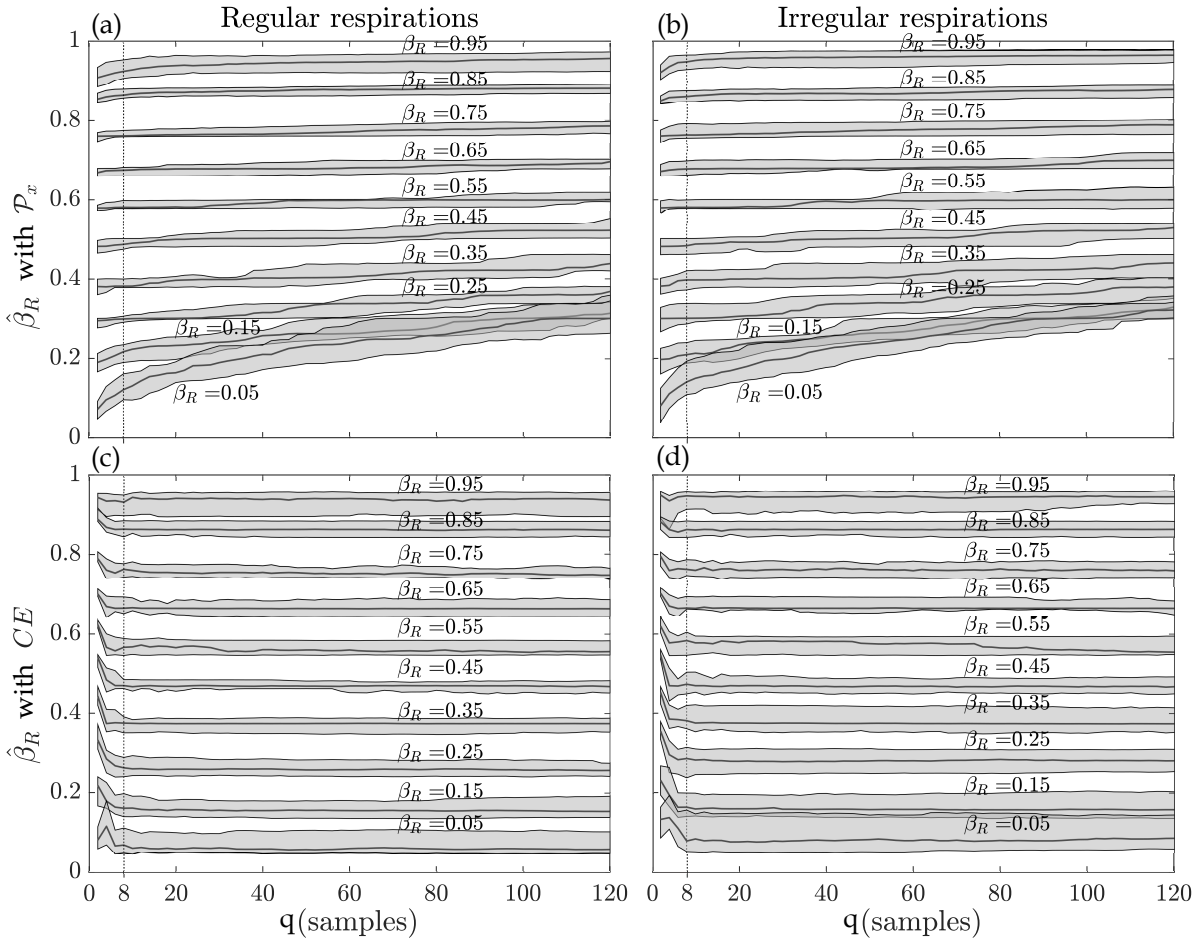

Figure 4. Effect of the model order in the predicted $\hat{\beta}_R$. (a) and (b) are made for $\mathcal{P}_x$ with regular and irregular respiratory segments, respectively. (c) and (d) are made for CE with regular and irregular respiratory segments, respectively. The real (β_R) and the estimated ($\hat{\beta}_R$) coupling are indicated for each simulation. The means and interquartile range (shaded areas) are shown. The black dotted line indicates a model order of 8, point after which the obtained RSA estimates are consistent.

that the standard deviation of the differences for $\mathcal{P}_x$ increases with the model order. The figure confirms that this effect is more noticeable when a weak coupling occurs. For CE, on the other hand, the standard deviation of the differences remains relatively constant. To visualize the change of σ in the Bland-Altman plots, it was calculated for all the model orders. Figure 6 shows the results. A relationship between q and σ is clearly observed for $\mathcal{P}_x$. With CE, the change with different model orders is not evident. To complement these results, the model order q'_* in which the quantification became significantly different to the computation with $q = 8$ was found. Table 1 shows the results. The subindex indicates if the calculations involved regular or irregular respiratory segments. It is seen that from a model order of 20, a significantly higher $\mathcal{P}_x$ is obtained in weakly coupled signals. For CE, the estimation was never significantly different.

To have an idea of the meaning of the results presented so far, the application to

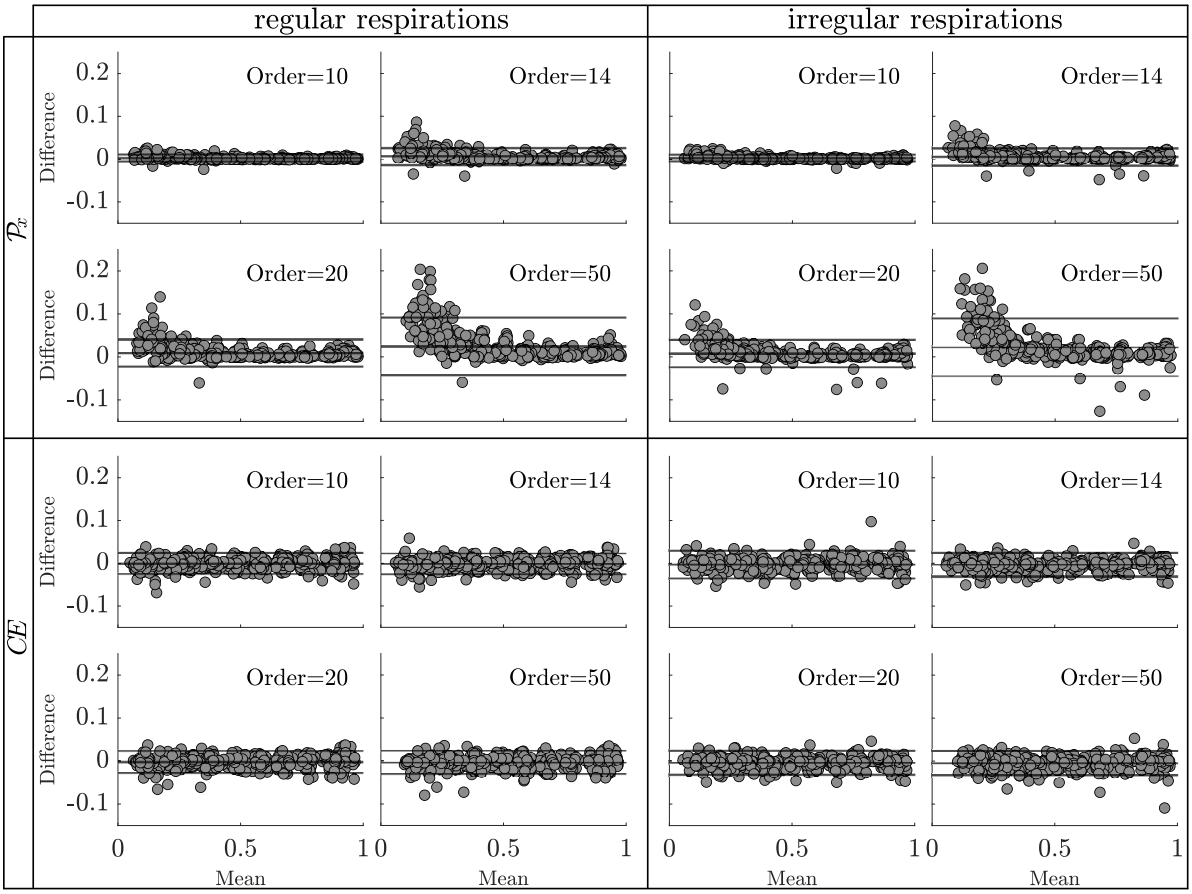

Figure 5. Bland-Altman plots for different model order. Each column indicates the use of either regular o irregular respiratory segments. The top plots correspond to $\mathcal{P}_x$ and the bottom to CE. The model order used for each plot is indicated.

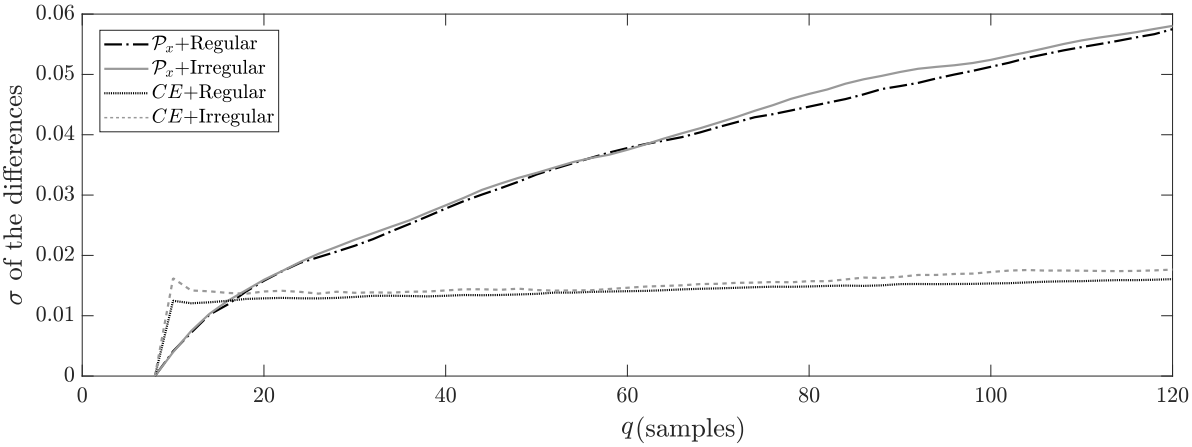

Figure 6. Change of standard deviation in the Bland-Altman plots as function of the model orders.

	$\mathcal{P}_x$		CE	
β_R	q'_r	q'_{irr}	q'_r	q'_{irr}
0.9-1.0	-	-	-	-
0.8-0.9	100	-	-	-
0.7-0.8	90	120	-	-
0.6-0.7	96	98	-	-
0.5-0.6	70	-	-	-
0.4-0.5	56	80	-	-
0.3-0.4	48	80	-	-
0.2-0.3	32	48	-	-
0.1-0.2	30	30	-	-
0.0-0.1	20	28	-	-

Table 1. Model orders in which the estimates become significantly different to the case in which $q = 8$. The subscripts r and irr stand for regular and irregular, respectively.

real data in [13] can be used. Here, the cardiorespiratory coupling was quantified for different sleep stages using a dataset of healthy patients. Differences were found between non rapid eye movement 1 (NEREM1), NREM2 and NREM3, with median $\hat{\beta}_R$ of 0.36, 0.4 and 0.44, respectively using $\mathcal{P}_x$. This application shows that such coupling levels occur and an incorrect selection of the model order for the calculation of $\mathcal{P}_x$ might have an important impact in the drawn conclusions. This is confirmed when looking at the change of σ in the Bland Altman plots in Figure 6. In this plot, for example when $q = 40$, σ goes up to 0.03. This means that if different model orders up to 40 had been used in [13], the wrong coupling level would have been estimated and significant differences between sleep stages would not have been found.

Finally, the different criteria for model order selection, q, were analyzed. Figure 7 shows the histograms of the selected q in each case for the computation with CE. The results for $\mathcal{P}_x$ are very similar and are not shown. In general, MDL chooses smaller values than AIC and the empirical approach. In addition, when the coupling between the signals is increased, MDL and AIC tend to select a smaller q compared to the case of a weak coupling. The empirical approach, on the other hand, shows the same trends for any coupling level and in general chooses $q \approx 80$. From these results, it can be said that MDL had a better performance because it chooses lower model orders, and these are more consistent over different realizations. In any case, this figure shows the discrepancy between the different criteria for model order selection.

In Figure 4, it is observed that $q > 5$ for CE and $q < 15$ for $\mathcal{P}_x$ are values that result in estimations of the RSA that are able to distinguish between different coupling levels. For this reason, these values are considered a good selection for the model order. Accordingly, the experiments in the rest of the paper were done using a unique model order of 2.5 seconds (10 samples) for both estimates.

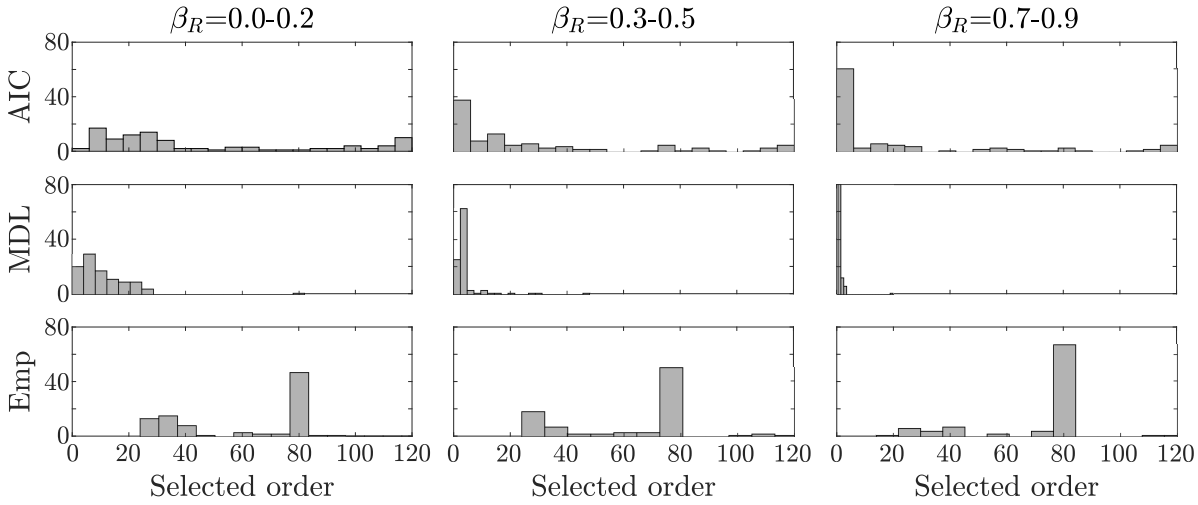

Figure 7. Histograms for the model orders selected with MDL, AIC and the empirical approaches for different coupling levels. The results are for the computation of CE. The results with $\mathcal{P}_x$ are very similar. Hence, they are not shown in the Figure.

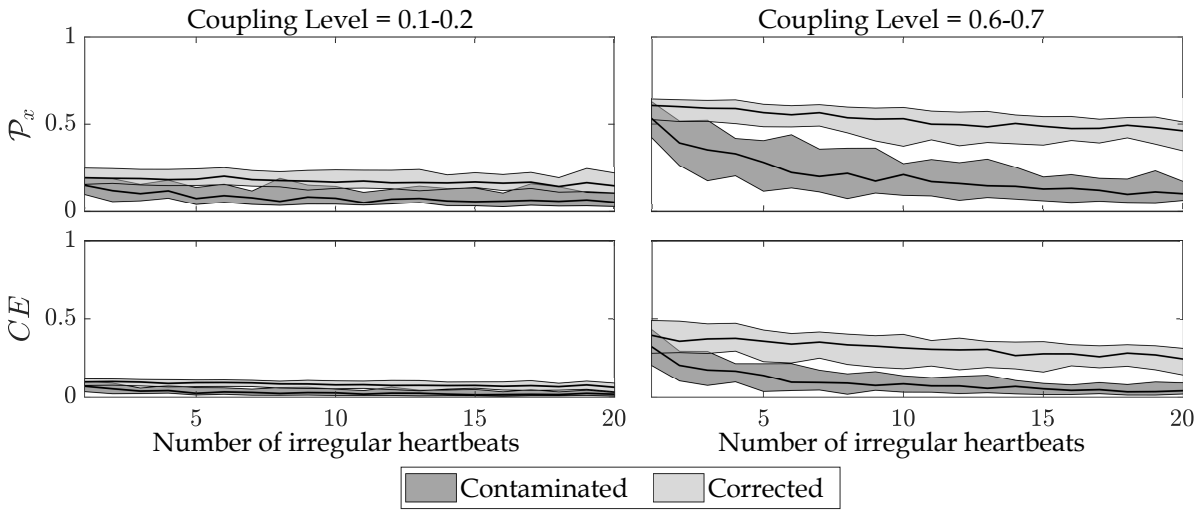

Figure 8. Effect of irregularities in the RSA estimates.

3.2. Effect of irregular heartbeats

Figure 8 shows the results with the RSA estimates when different amounts of irregular heartbeats are added to the signals. Both estimates behave similarly in the sense that when the coupling is weak, the effect is less noticeable. In contrast, when the coupling is stronger, and even with an irregular heartbeat correction step (i.e., detection and interpolation), both RSA estimates are significantly affected.

Figure 9 shows the change of the standard deviation of the differences in the Bald-Altman plots when different number of irregular heartbeats are allowed. As expected from the results in Figure 8, there is a linear increasing relationship between the number of irregular heartbeats and σ. Notice that, even after a step of correction, the increasing trend is present and it is similar with both estimates. Table 2 depicts the number of

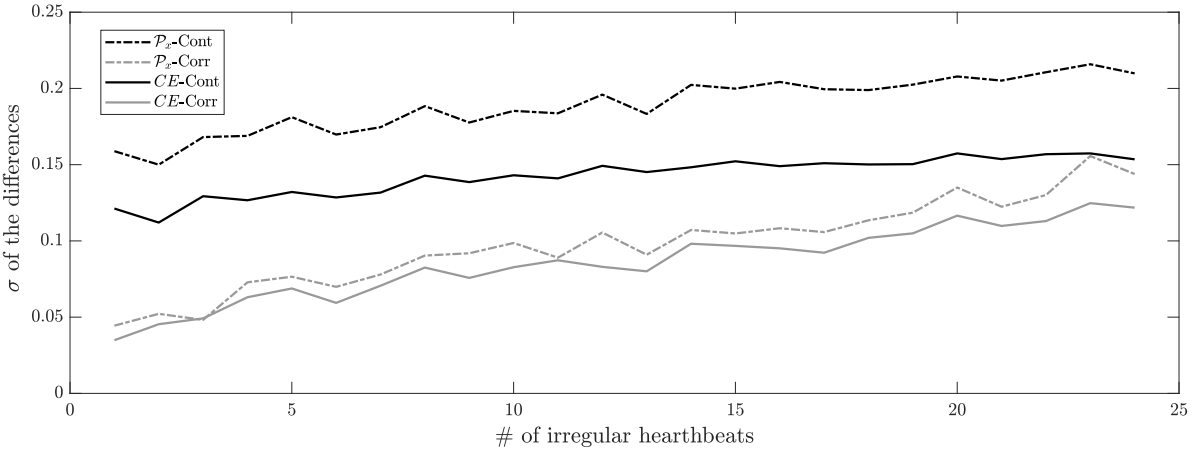

Figure 9. Change of σ for the differences in the Bald-Altman plots for different number of irregular heartbeats.

	$\mathcal{P}_x$		CE	
	# Irregulars		**# Irregulars**	
Actual $\mathcal{P}_x$	Cont	Corr	Cont	Corr
0.0-0.1	3	11	3	10
0.1-0.2	3	13	3	9
0.2-0.3	3	11	3	11
0.3-0.4	2	10	3	11
0.4-0.5	3	10	3	10
0.5-0.6	3	7	3	11
0.6-0.7	2	5	2	7
0.7-0.8	2	6	2	7
0.8-0.9	2	5	2	6

Table 2. Tests for the effect of irregular beats in the quantification of the RSA with $\mathcal{P}_x$ and CE. # irregulars indicates the number of irregular heartbeats in which the RSA estimates become significantly different to the irregular-free case. The analyses are done for the contaminated (Cont) and corrected (Corr) signals.

irregular heartbeats in which the estimates become significantly different to the clean case. This table shows that, without a step of irregular heartbeats correction, the RSA estimates are already significantly different to the clean case after having only 2 irregular heartbeats. This occurs because the trends in the HRV representation change and both estimates depend on these trends to work properly. Furthermore, it is seen that the number of irregular heartbeats in which the RSA estimates become significantly different to the irregular-free case depends on the strength of the coupling. In any case, even after a correction step, the values are significantly different when 5 or more irregular heartbeats occur, if the coupling between the signals is strong.

Similarly to the model order selection, the application to real data in [13] can be used to have an idea of the magnitude of the errors. Figure 9 shows that, even after

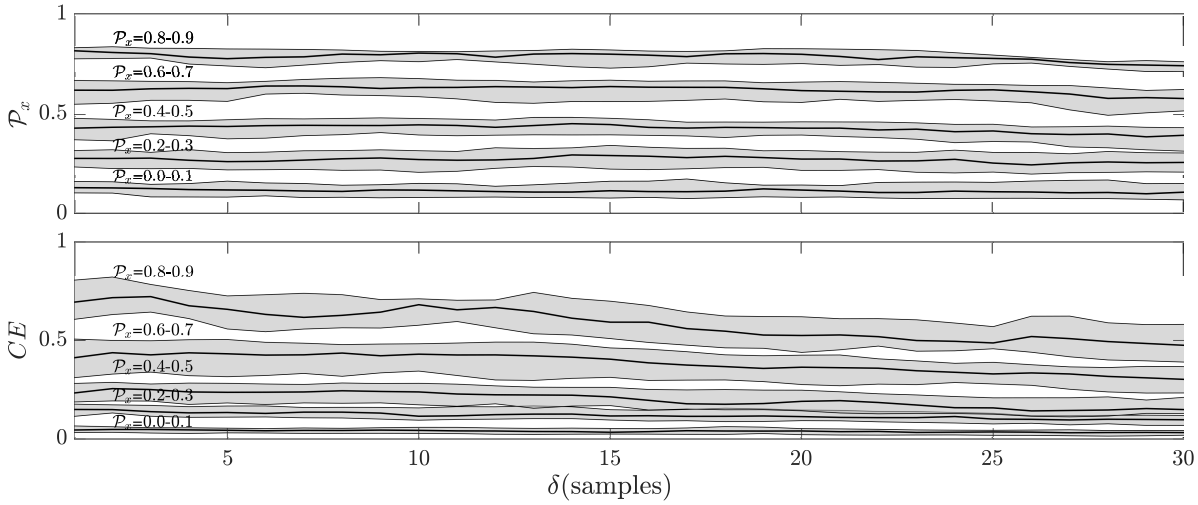

Figure 10. Effect of introducing delays between the HRV and respiratory signals on the RSA quantification using $\mathcal{P}_x$ and CE.

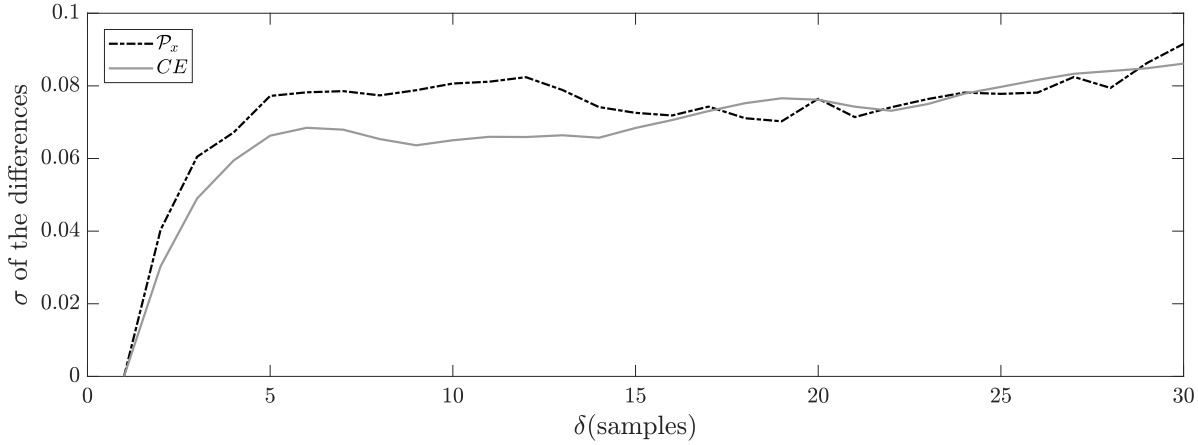

Figure 11. σ of the differences in the BaldAltman plots with different delays.

correcting for irregular heartbeats, allowing around 6 irregular produces $\sigma \approx 0.05$ with both methods. This means that if irregular heartbeats had occurred in [13], it would not have been possible to distinguish between different sleep stages.

3.3. Effect of delays

Figure 10 shows the effect of the delays, δ, in the RSA estimates. The change is more noticeable with CE than with $\mathcal{P}_x$, in particular for stronger coupling levels. A weak inverse relationship between both estimates and the delay in samples is observed. In any case, it is always possible to distinguish between different coupling levels.

Figure 11 shows the change of the σ of the differences of the Bland Altman plots for increased number of delays. An increasing trend is observed for $\delta \in [0\ 5]$. For larger delays, it does not change, suggesting that both estimates are relatively robust to the delays. Table 3 shows the delay in number of samples, δ', in which the estimates become

$\mathcal{P}_x$	$\mathcal{P}_x$ δ'	CE δ'
0.0-0.1	-	27
0.1-0.2	-	23
0.2-0.3	-	22
0.3-0.4	-	-
0.4-0.5	-	23
0.5-0.6	-	24
0.6-0.7	-	25
0.7-0.8	-	24
0.8-0.9	27	34

Table 3. Effect of the delays in the quantification of the RSA with $\mathcal{P}_x$ and CE. δ' indicates the number of samples in which the delay results in a significantly different RSA estimate compared to the non-delayed case.

significantly different to the zero delay case. From this table, it is seen that $\mathcal{P}_x$ is less affected than CE. However, δ' is always longer than 5 seconds, or 20 samples.

3.4. Effect of phase changes

Figure 12 shows the change of $\mathcal{P}_x$ and CE when a change of phase between the signals occurs over time. The plots are very similar for all coupling levels. The figure displays the case of a coupling between 0.4 and 0.5, as an example. Three surfaces are shown in each case, which correspond to the median value and the limits of the interquartile range. It is observed that, when the change of phase is up to 54°, the effect in the RSA estimates is almost never significant, no matter the duration of this phase change. After 54°, the significance of this effect in the quantification depends on the duration of the phase shift, with a stronger effect when this is of 60 seconds or longer. After 60 seconds and 54°, the RSA estimates are always significantly different ($\mathbf{p} < 0.05$) to the case in which a phase distortion is not introduced.

Figure 13 shows the increasing trend of the σ in the Bland-Altman plots when the duration/amplitude of the phase changes increase. The duration of the pulse was limited to 160 seconds because afterwards it was longer than half of the total duration of the segment.

3.5. Discussion

The goal of this paper was to assess the use of subspace projections and crossentropy to quantify the RSA. First, the effect of the model order in the calculations is tested. Then, the estimates are applied to three simulated scenarios that can occur in non controlled environments or in recordings from patient populations. More specifically, the analyses included the occurrence of irregular heartbeat, the delays between the signals and the

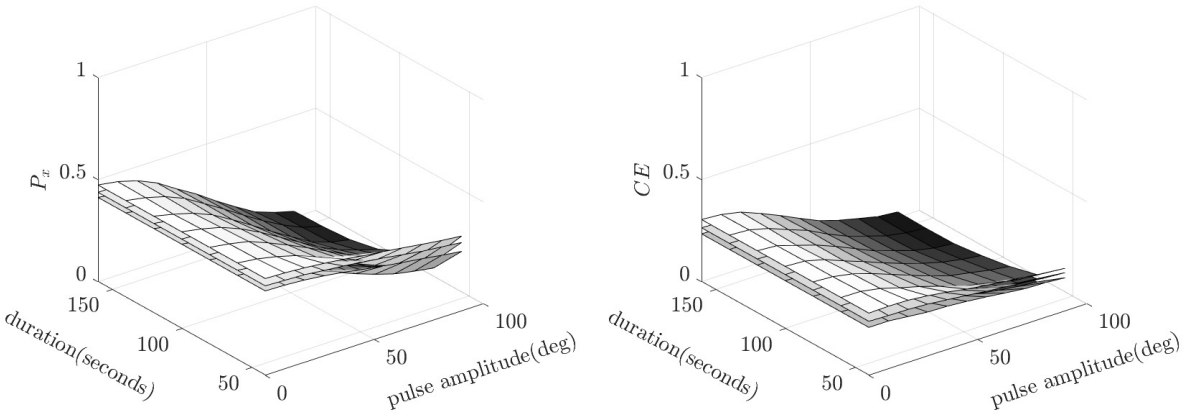

Figure 12. Effect of the phase changes between the HRV and respiratory signals on the RSA quantification using $\mathcal{P}_x$ and CE. The Figure shows the case in which the coupling level is between 0.4 and 0.5. The surfaces indicate the mean and interquartile ranges.

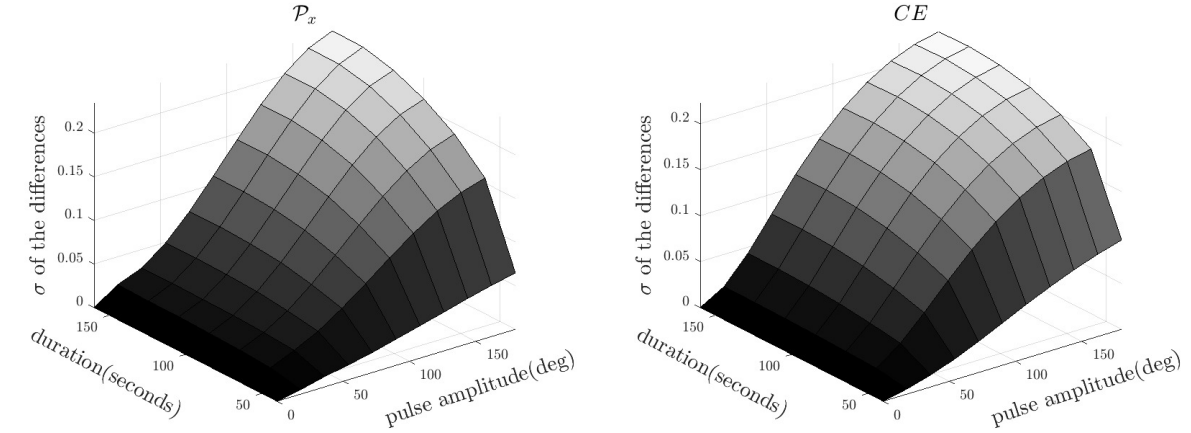

Figure 13. Change of the σ of the differences in the Bland-Altman plots for phase changes of different duration and amplitude.

changes of phase. This section discusses the results. To the best of the knowledge of the authors, these scenarios have not been studied in the context of RSA estimation.

3.5.1. Model order selection: $\mathcal{P}_x$ was more affected by the model order selection than CE. To understand this, it is important to explain that, similarly to CE, the calculation of $\mathcal{P}_x$ can be seen as the result of fitting a regression model to predict the HRV in function of the past of the respiration. The coefficients of this regression are given by the projection matrix $\mathbf{P}$, which considers the whole dynamics of the respiration. This is not the case for CE, which only considers q past samples, reducing the likelihood of overfitting. This makes $\mathcal{P}_x$ more prone to overfitting problems if q is bigger than needed and this effect is more noticeable when a weak coupling between the signals occurs. A stronger coupling results on more significant coefficients for the regression.
Regarding the criteria for model order selection, it was seen that, in general, lower

coupling levels need higher model orders. These criteria try to find the model order that better fits the data with the lowest possible complexity. In cases in which the coupling is weak, the relationship between the past of the respiration and the present samples of the HRV is more difficult to find. This produces regression models with less significant coefficients. Hence, the addition of more coefficients for the regression, which translates into a higher model order, represents an improvement to fit the data.
The problem of order selection for MVAR models is not new. Each researcher tackles this issue in different ways. The paper in [40] proposes a novel approach based on an iterative optimization which is used to characterize electroencephalographic recordings. In [41], an MVAR model is used to investigate if the inverse pulse time series could replace the systolic blood pressure signal. MDL gave an initial q that was then refined by analyzing the most significant coefficients in the regression. The work in [42] analyses the causal interactions between electrodermal activity and HRV using an MVAR in which q was tuned using an approach based on AIC. In the specific case of cardiorespiratory coupling, the work presented in [32] highlights the need to standardize the selection of q to facilitate the interpretability and usability of MVAR model-based methods. In [6], q is calculated, depending on the characteristics of the respiratory signal, as the minimum or maximum between MDL and AIC. In [13], it was found that MDL and AIC resulted on very different model orders. Hence, an empirical approach based on the spectral characteristics of the respiratory signals was proposed. The results from the simulations done in the current work suggest that q can take a unique value. In this way, the obtained estimate will reflect the actual coupling level between the HRV and respiration.

At this point, it is important to mention that the final goal of the order selection for the quantification of the cardiorespiratory coupling is not to produce a model that better fits the data, but to obtain an RSA estimate able to reflect the actual coupling level. Under this premise, and according to the results presented, a single model order works well when clean segments are used. In any case, the analyses with $\mathcal{P}_x$ is more sensitive to the model order selection compared to CE, in particular when a weak coupling occurs.

3.5.2. Irregular heartbeats: The presence of irregular heartbeats in the ECG signals is problematic for HRV analyses. In [8], this is highlighted and it is recommended to apply proper interpolation techniques to correct for them. In addition, the study in [15] showed that despite the fact that beat replacement reduced the errors in the estimation of HRV indexes in the frequency domain, these were still affected even with a low number of irregularities. These results are confirmed in [43], where the analyses are extended to HRV indexes in the time domain. These works show that irregular heartbeats significantly affect HRV indexes and the same would be expected for the cardiorespiratory parameters.
The simulation results show that the irregular heartbeats have an important influence on the RSA estimates. In addition, and in line with the literature for HRV variability, even after a step of irregular heartbeat correction the estimates are significantly affected

after allowing 5 or more irregular heartbeats in a period of 5 minutes. The application and interpretation of CE and $\mathcal{P}_x$ in these cases must be done carefully.

3.5.3. Delay: The authors in [44] and [45] used the maximum of the cross correlation function in a window of 3 seconds to evaluate the accuracy of methods for ECG derived respiration (EDR). This is done to correct for possible delays between the EDR and the actual respiratory signals. Also, in [18] it is shown that depending on the electrode configuration, the delays between the respiratory volume and the bioimpedance signal is different. For RSA estimation, different modalities can be used as respiratory signal. Examples include belts, the impedance plethysmography, the EDR or the bioimpedance. The aforementioned papers suggest that these signals might be delayed differently with respect to the HRV. As a result, the quantification of the cardiorespiratory coupling might also be different depending on the used modality. The current paper tested this hypothesis.
The results of the simulations suggest that the delays do not have a strong impact on the RSA estimates. This result is due to the fact that the respiratory signals have a repetitive pattern, which facilitates the fitting of the models to calculate the estimates. This repetitiveness is intrinsic of the respiratory signals and it occurs even when they have irregular patterns. It was observed that CE was significantly different to the no delayed case with a smaller delay compared to $\mathcal{P}_x$. Similarly to the selection of the model order, an explanation for this observation is that the calculation of the projection matrix $\mathbf{P}$ for $\mathcal{P}_x$ considers the dynamics of the respiration in the whole segment. This is not the case for CE, which only considers q past samples. Hence, CE is more likely to be affected by the delays. However, the number of delays in which significant differences were found in the simulations was always higher than 5 seconds, when in practice such long delays are not expected. For this reason, correcting the delays is not essential for the calculations.

3.5.4. Change of phase In diseases such as sleep apnea [46] or chronic obstructive pulmonary disease [47], paradoxical respiration can happen. This is an example of a real case in which a phase change between the HRV and the respiration will occur. In addition, as mentioned in the introduction, changes in the phase locking between both signals have been reported in the literature. For these reasons, it is important to study the effect of these changes in the RSA estimates. The results from the simulations show that the extend in which the estimates are affected by phase changes depends on their duration and amplitude. This occurs because $\mathcal{P}_x$ and CE are linear approaches. As such, they need stationary segments and a linear correlation maintained over the duration of the recording to properly capture the strength of the RSA. These methods should be adapted to be computed in short windows and continuously in order to work well in cases in which phase changes occur.

4. Conclusions

This paper evaluated the use of orthogonal subspace projections and crossentropy to estimate the strength of the RSA in different scenarios. The results identify pitfalls of state-of-the art methods when used in real conditions. Directions on how to perform optimal analysis and interpretation of results in future applications are given. For the model order, a single value higher than 5 for crossentropy or lower than 15 for orthogonal subspace projections produced consistent estimations. In case of irregular heartbeats, the results suggest that the interpretation should be careful if 5 or more irregulars occur in a 5-minute epoch, even after a step of irregular heartbeats correction. For the delay, orthogonal subspace projections were less affected than crossentropy, but both estimates are robust. Regarding the phase between the signals, a change of 54° lasting more than one fifth the duration of the recording significantly affected the estimates.

Acknowledgments

BOF, C24/18/097. VLAIO, 150466: OSA+. EU H2020 MSCA-ITN-2018: (INSPiRE-MED) #813120. EU H2020 MSCA-ITN-2018: (INFANS) #813483. EIT Health—SeizeIT2 19263. This research received funding from the Flemish Government (AI Research Program). KU Leuven Stadius acknowledges the financial support of imec.

References

[1] W. Hrushesky, D. Fader, O. Schmitt, and V. Gilbertsen, "The respiratory sinus arrhythmia: a measure of cardiac age," *Science*, vol. 224, no. 4652, pp. 1001–1004, 1984.

[2] J. D. Mackay, "Respiratory sinus arrhythmia in diabetic neuropathy," *Diabetologia*, vol. 24, pp. 253–256, Apr 1983.

[3] M. R. Bonsignore, S. Romano, O. Marrone, and G. Insalaco, "Respiratory sinus arrhythmia during obstructive sleep apnoeas in humans," *Journal of Sleep Research*, vol. 4, no. s1, pp. 68–70, 1995.

[4] M. Peltola, M. P. Tulppo, A. Kiviniemi, A. J. Hautala, T. Seppänen, P. Barthel, A. Bauer, G. Schmidt, H. V. Huikuri, and T. H. Mäkikallio, "Respiratory sinus arrhythmia as a predictor of sudden cardiac death after myocardial infarction," *Annals of Medicine*, vol. 40, no. 5, pp. 376–382, 2008.

[5] S. M. Gorka, S. K. McGowan, M. L. Campbell, B. D. Nelson, C. Sarapas, J. R. Bishop, and S. A. Shankman, "Association between respiratory sinus arrhythmia and reductions in startle responding in three independent samples," *Biological Psychology*, vol. 93, no. 2, pp. 334–341, 2013.

[6] C. Varon, J. Lázaro, J. Bolea, A. Hernando, J. Aguiló, E. Gil, S. Van Huffel, and R. Bailón, "Unconstrained estimation of HRV indices after removing respiratory influences from heart rate," *IEEE Journal of Biomedical and Health Informatics*, vol. 23, no. 6, pp. 2386–2397, 2019.

[7] L. Sörnmo and P. Laguna, "Chapter 8 - ecg signal processing: Heart rate variability," in *Bioelectrical Signal Processing in Cardiac and Neurological Applications* (L. Sörnmo and P. Laguna, eds.), Biomedical Engineering, pp. 567–631, Burlington: Academic Press, 2005.

[8] A. J. Camm, M. Malik, J. T. Bigger, G. Breithardt, S. Cerutti, R. J. Cohen, P. Coumel, E. L. Fallen, H. L. Kennedy, R. Kleiger, *et al.*, "Heart rate variability: standards of measurement, physiological interpretation and clinical use. task force of the european society of cardiology and the north american society of pacing and electrophysiology," 1996.

[9] T. E. Brown, L. A. Beightol, J. Koh, and D. L. Eckberg, "Important influence of respiration on human RR interval power spectra is largely ignored," *Journal of Applied Physiology*, vol. 75, no. 5, pp. 2310–2317, 1993.

[10] J. Schipke, G. Arnold, and M. Pelzer, "Effect of respiration rate on short-term heart rate variability," *Journal of Clinical and Basic Cardiology*, vol. 2, no. 1, pp. 92–95, 1999.

[11] E. O'Callaghan, R. Lataro, L. Zhao, A. Ben-Tal, A. Nogaret, and J. Paton, "Cardiac output is improved in rats with myocardial infarction by enhancement of respiratory sinus arrhythmia," *The FASEB Journal*, vol. 29, no. 1_supplement, pp. 1043–3, 2015.

[12] T. M. Shader, L. M. Gatzke-Kopp, S. E. Crowell, M. J. Reid, J. F. Thayer, M. W. Vasey, C. Webster-Stratton, Z. Bell, and T. P. Beauchaine, "Quantifying respiratory sinus arrhythmia: Effects of misspecifying breathing frequencies across development," *Development and psychopathology*, vol. 30, no. 1, pp. 351–366, 2018.

[13] J. Morales, J. Moeyersons, P. Armanac, M. Orini, L. Faes, S. Overeem, M. Van Gilst, J. Van Dijk, S. Van Huffel, R. Bailon, and C. Varon, "Model-based evaluation of methods for respiratory sinus arrhythmia estimation," *IEEE Transactions on Biomedical Engineering*, pp. 1–1, 2020.

[14] L. Faes, A. Porta, and G. Nollo, "Information decomposition in bivariate systems: Theory and application to cardiorespiratory dynamics," *Entropy*, vol. 17, no. 1, pp. 277–303, 2015.

[15] G. D. Clifford and L. Tarassenko, "Quantifying errors in spectral estimates of HRV due to beat replacement and resampling," *IEEE Transactions on Biomedical Engineering*, vol. 52, no. 4, pp. 630–638, 2005.

[16] S. Abe, M. Yoshizawa, N. Nakanishi, T. Yazawa, K. Yokota, M. Honda, and G. Sloman, "Electrocardiographic abnormalities in patients receiving hemodialysis," *American Heart Journal*, vol. 131, pp. 1137–1144, Jun 1996.

[17] A. S. Hersi, "Obstructive sleep apnea and cardiac arrhythmias," *Annals of thoracic medicine*, vol. 5, pp. 10–17, Jan 2010.

[18] D. Blanco-Almazán, W. Groenendaal, F. Catthoor, and R. Jané, "Analysis of time delay between bioimpedance and respiratory volume signals under inspiratory loaded breathing," in *2019 41st Annual International Conference of the IEEE Engineering in Medicine and Biology Society (EMBC)*, pp. 2365–2368, 2019.

[19] M. G. Rosenblum, A. S. Pikovsky, and J. Kurths, "Phase synchronization of chaotic oscillators," *Phys. Rev. Lett.*, vol. 76, pp. 1804–1807, Mar 1996.

[20] C. E. Mazzucco, A. Marchi, V. Bari, B. De Maria, S. Guzzetti, F. Raimondi, E. Catena, D. Ottolina, C. Amadio, S. Cravero, *et al.*, "Mechanical ventilatory modes and cardioventilatory phase synchronization in acute respiratory failure patients," *Physiological measurement*, vol. 38, no. 5, p. 895, 2017.

[21] J. Solà-Soler, B. F. Giraldo, J. A. Fiz, and R. Jané, "Cardiorespiratory phase synchronization in OSA subjects during wake and sleep states," in *2015 37th Annual International Conference of the IEEE Engineering in Medicine and Biology Society (EMBC)*, pp. 7708–7711, 2015.

[22] M. Lucchini, N. Pini, W. P. Fifer, N. Burtchen, and M. G. Signorini, "Characterization of cardiorespiratory phase synchronization and directionality in late premature and full term infants," *Physiological Measurement*, vol. 39, no. 6, p. 064001, 2018.

[23] J. Mateo and P. Laguna, "Improved heart rate variability signal analysis from the beat occurrence times according to the ipfm model," *IEEE Transactions on Biomedical Engineering*, vol. 47, no. 8, pp. 985–996, 2000.

[24] N. Iyengar, C. K. Peng, R. Morin, A. L. Goldberger, and L. A. Lipsitz, "Age-related alterations in the fractal scaling of cardiac interbeat interval dynamics," *American Journal of Physiology-Regulatory, Integrative and Comparative Physiology*, vol. 271, no. 4, pp. R1078–R1084, 1996.

[25] J. Healey and R. Picard, "Detecting stress during real-world driving tasks using physiological sensors," *IEEE Transactions on Intelligent Transportation Systems*, vol. 6, no. 2, pp. 156–166, 2005.

[26] M. Deviaene, P. Borzée, M. van Gilst, J. van Dijk, S. Overeem, B. Buyse, D. Testelmans, S. Van

Huffel, and C. Varon, "Multilevel interval coded scoring to assess the cardiovascular status of sleep apnea patients using oxygen saturation markers," *IEEE Transactions on Biomedical Engineering*, vol. 67, no. 10, pp. 2839–2848, 2020.

[27] E. J. Bayly, "Spectral analysis of pulse frequency modulation in the nervous systems," *IEEE Transactions on Biomedical Engineering*, vol. BME-15, no. 4, pp. 257–265, 1968.

[28] R. W. Jones, C. C. Li, A. U. Meyer, and R. B. Pinter, "Pulse modulation in physiological systems, phenomenological aspects," *IRE Transactions on Bio-Medical Electronics*, vol. 8, no. 1, pp. 59–67, 1961.

[29] C. Varon, A. Caicedo, D. Testelmans, B. Buyse, and S. Van Huffel, "A novel algorithm for the automatic detection of sleep apnea from single-lead ECG," *IEEE Transactions on Biomedical Engineering*, vol. 62, no. 9, pp. 2269–2278, 2015.

[30] R. B. Berry, R. Budhiraja, D. J. Gottlieb, D. Gozal, C. Iber, V. K. Kapur, C. L. Marcus, R. Mehra, S. Parthasarathy, S. F. Quan, *et al.*, "Rules for scoring respiratory events in sleep: update of the 2007 AASM manual for the scoring of sleep and associated events," *Journal of clinical sleep medicine*, vol. 8, no. 05.

[31] J. Morales, P. Borzee, D. Testelmans, B. Buyse, S. Van Huffel, and C. Varon, "Linear and non-linear quantification of the respiratory sinus arrhythmia using support vector machines," *Frontiers in Physiology*, vol. 12, p. 58, 2021.

[32] S. Schulz, F.-C. Adochiei, I.-R. Edu, R. Schroeder, H. Costin, K.-J. Bär, and A. Voss, "Cardiovascular and cardiorespiratory coupling analyses: a review," *Philosophical Transactions of the Royal Society A: Mathematical, Physical and Engineering Sciences*, vol. 371, no. 1997, p. 20120191, 2013.

[33] H. Akaike, "A new look at the statistical model identification," *IEEE Transactions on Automatic Control*, vol. 19, no. 6, pp. 716–723, 1974.

[34] J. Rissanen, "Modeling by shortest data description," *Automatica*, vol. 14, no. 5, pp. 465–471, 1978.

[35] J. Morales, P. Borzée, D. Testelmans, B. Buyse, S. Van Huffel, R. Bailón, and C. Varon, "A robust estimation of the cardiorespiratory coupling in the presence of abnormal beats," in *2020 Computing in Cardiology*, pp. 1–4, 2020.

[36] P. M. Lehrer, E. G. Vaschillo, and V. Vidali, "Heart rate and breathing are not always in phase during resonance frequency breathing," *Applied psychophysiology and biofeedback*, vol. 45, no. 3, pp. 145–152, 2020.

[37] C. Schäfer, M. G. Rosenblum, J. Kurths, and H.-H. Abel, "Heartbeat synchronized with ventilation," *Nature*, vol. 392, pp. 239–240, Mar 1998.

[38] M. G. Rosenblum, A. S. Pikovsky, and J. Kurths, "Phase synchronization of chaotic oscillators," *Phys. Rev. Lett.*, vol. 76, pp. 1804–1807, Mar 1996.

[39] D. Giavarina, "Understanding bland altman analysis," *Biochemia medica*, vol. 25, no. 2, pp. 141–151, 2015.

[40] D. M. Khan, N. Yahya, and N. Kamel, "Optimum order selection criterion for autoregressive models of bandlimited EEG signals," in *2020 IEEE-EMBS Conference on Biomedical Engineering and Sciences (IECBES)*, pp. 389–394, 2021.

[41] P. Giassi, S. Okida, M. G. Oliveira, and R. Moraes, "Validation of the inverse pulse wave transit time series as surrogate of systolic blood pressure in MVAR modeling," *IEEE Transactions on Biomedical Engineering*, vol. 60, no. 11, pp. 3176–3184, 2013.

[42] A. L. Callara, L. Sebastiani, N. Vanello, E. P. Scilingo, and A. Greco, "Parasympathetic-sympathetic causal interactions assessed by time-varying multivariate autoregressive modeling of electrodermal activity and heart-rate-variability," *IEEE Transactions on Biomedical Engineering*, pp. 1–1, 2021.

[43] A. Choi and H. Shin, "Quantitative analysis of the effect of an ectopic beat on the heart rate variability in the resting condition," *Frontiers in Physiology*, vol. 9, p. 922, 2018.

[44] C. Varon, J. Morales, J. Lázaro, M. Orini, M. Deviaene, S. Kontaxis, D. Testelmans, B. Buyse,

P. Borzée, L. Sörnmo, P. Laguna, E. Gil, and R. Bailón, "A comparative study of ECG-derived respiration in ambulatory monitoring using the single-lead ECG," *Scientific Reports*, vol. 10, p. 5704, Mar 2020.

[45] "Sleep apnea detection from single-lead ecg using features based on ECG-derived respiration (EDR) signals," *IRBM*, vol. 39, no. 3, pp. 206–218, 2018.

[46] W. J. Randerath, M. Treml, C. Priegnitz, S. Stieglitz, L. Hagmeyer, and C. Morgenstern, "Evaluation of a Noninvasive Algorithm for Differentiation of Obstructive and Central Hypopneas," *Sleep*, vol. 36, pp. 363–368, 03 2013.

[47] A. Aliverti, M. Quaranta, B. Chakrabarti, A. L. P. Albuquerque, and P. M. Calverley, "Paradoxical movement of the lower ribcage at rest and during exercise in copd patients," *European Respiratory Journal*, vol. 33, no. 1, pp. 49–60, 2009.